Integrated analysis of gray and white matter alterations in attention-deficit/hyperactivity disorder

Winke Francx[a,b,*], Alberto Llera[b,1], Maarten Mennes[b,1], Marcel P. Zwiers[a,b], Stephen V. Faraone[g,h], Jaap Oosterlaan[c], Dirk Heslenfeld[c], Pieter J. Hoekstra[d], Catharina A. Hartman[d], Barbara Franke[i,j], Jan K. Buitelaar[a,b,e,2], Christian F. Beckmann[a,b,f,2]

[a]Radboud University Medical Center, Donders Institute for Brain, Cognition and Behaviour, Nijmegen, Department of Cognitive Neuroscience, Nijmegen, The Netherlands
[b]Radboud University Nijmegen, Donders Institute for Brain, Cognition and Behaviour, Centre for Cognitive Neuroimaging, Nijmegen, The Netherlands
[c]VU University Amsterdam, Department of Clinical Neuropsychology, Amsterdam, The Netherlands
[d]University of Groningen, University Medical Center Groningen, Department of Psychiatry, Groningen, The Netherlands
[e]Karakter Child and Adolescent Psychiatry University Centre, Nijmegen, The Netherlands
[f]Centre for Functional MRI of the Brain, University of Oxford, Oxford, United Kingdom
[g]Departments of Psychiatry and of Neuroscience and Physiology, SUNY Upstate Medical University, Syracuse, USA
[h]K.G. Jebsen Centre for Psychiatric Disorders, Department of Biomedicine, University of Bergen, Bergen, Norway
[i]Radboud University Medical Center, Donders Institute for Brain, Cognition and Behaviour, Nijmegen, Department of Human Genetics, Nijmegen, The Netherlands
[j]Radboud University Nijmegen, Donders Institute for Brain, Cognition and Behaviour, Department of Psychiatry, Nijmegen, The Netherlands

ARTICLE INFO

ABSTRACT

Background: Magnetic resonance imaging (MRI) is able to provide detailed insights into the structural organization of the brain, e.g., by means of mapping brain anatomy and white matter microstructure. Understanding interrelations between MRI modalities, rather than mapping modalities in isolation, will contribute to unraveling the complex neural mechanisms associated with neuropsychiatric disorders as deficits detected across modalities suggest common underlying mechanisms. Here, we conduct a multimodal analysis of structural MRI modalities in the context of attention-deficit/hyperactivity disorder (ADHD).

Methods: Gray matter volume, cortical thickness, surface areal expansion estimates, and white matter diffusion indices of 129 participants with ADHD and 204 participants without ADHD were entered into a linked independent component analysis. This data-driven analysis decomposes the data into multimodal independent components reflecting common inter-subject variation across imaging modalities.

Results: ADHD severity was related to two multimodal components. The first component revealed smaller prefrontal volumes in participants with more symptoms, co-occurring with abnormal white matter indices in prefrontal cortex. The second component demonstrated decreased orbitofrontal volume as well as abnormalities in insula, occipital, and somato-sensory areas in participants with more ADHD symptoms.

Conclusions: Our results replicate and extend previous unimodal structural MRI findings by demonstrating that prefrontal, parietal, and occipital areas, as well as fronto-striatal and fronto-limbic systems are implicated in ADHD. By including multiple modalities, sensitivity for between-participant effects is increased, as shared variance across modalities is modeled. The convergence of modality-specific findings in our results suggests that different aspects of brain structure share underlying pathophysiology and brings us closer to a biological characterization of ADHD.

1. Introduction

Attention-Deficit/Hyperactivity Disorder (ADHD) is a neurodevelopmental disorder that consistently has been related to abnormalities in brain structure. Magnetic resonance imaging (MRI) provides insights into brain morphology and white matter mesostructure by means of high-resolution anatomical imaging and diffusion-weighted imaging. To date, analyses have focused on each data modality separately, thus limiting conclusions to the modality analyzed. Recent

* Corresponding author at: Radboud University Nijmegen Medical Centre, Donders Institute for Brain, Cognition and Behaviour, Kapittelweg 29, 6525EN Nijmegen, The Netherlands.
  E-mail address: w.francx@donders.ru.nl (W. Francx).
[1] Both authors contributed equally.
[2] Shared last authorship.

advances in analytic techniques support integration of different data modalities, allowing for a simultaneous multimodal characterization of the biological markers associated with neuropsychiatric disorders (Groves et al., 2011).

Focusing on single data modalities, ADHD has been associated with decreased cortical thickness of regions implicated in attentional processing and cognitive control, including the frontal lobe and anterior cingulate cortex (ACC) (Castellanos et al., 2002; Narr et al., 2009). In addition, maturation of cortical thickness is delayed in ADHD compared to controls, with a maturational lag of up to five years in the prefrontal cortex (Shaw et al., 2007). Cortical surface area (relative amount of areal expansion or compression) exhibits a similar developmental delay (Shaw et al., 2012). Yet, although anomalies in prefrontal cortical thickness in ADHD are consistent, divergent findings outside the prefrontal cortex have been reported. These include thinner bilateral medial temporal cortices and increased cortical thickness in left superior parietal cortex (Narr et al., 2009).

Brain volumetric analyses have associated ADHD with a 3–5% smaller total brain and gray matter volume compared to controls (Castellanos et al., 2002; Greven et al., 2015). Further, voxel-based morphometry (VBM) analyses in ADHD support results of smaller prefrontal volumes, more specifically of ACC (Frodl & Skokauskas, 2012), and reveal smaller volumes across several specific brain regions, most consistently in basal ganglia, thalamus, cerebellum, and amygdala (Frodl & Skokauskas, 2012; Plessen et al., 2006; Mackie et al., 2007; Nakao et al., 2011).

Alterations in the brain's white matter have frequently been reported in ADHD. While diffusion indices describe different aspects of white matter microstructure (e.g., fractional anisotropy [FA]; mean diffusivity [MD]; tensor mode [MO]), studies concerning ADHD have mainly focused on FA. Yet, the reported findings have been heterogeneous and widespread throughout the brain, possibly because of region of interest approaches, variation in analysis techniques, and small sample sizes. A recent meta-analysis reported altered FA associated with ADHD in the tracts of the fronto-striatal-cerebellar circuit (van Ewijk et al., 2012).

The heterogeneity of imaging-based findings in ADHD, as described above, negatively impacts on our ability to interpret modality-specific results in the biological context of underlying pathophysiology. This is largely due to the isolated picture of brain abnormalities that is provided by unimodal univariate analyses. Recently developed analysis techniques allow integrative analyses across imaging modalities (Groves et al., 2011). Analyzing data in a multimodal way allows identification of co-occurring changes across brain measures, potentially reflecting shared pathophysiology and etiological processes. Importantly, this integrative approach does still allow for unimodal findings to be identified (Groves et al., 2012). Analyses integrating modalities add up to more than the sum of the modalities, as the integration of metrics increases sensitivity for between-participant effects by providing improved modeling of shared variance across modalities (Groves et al., 2012). While moving from uni- to multi-modal analysis permits the simultaneous characterization across different aspects of biological change measured by different MR modalities, the uni- to multi-variate change permits the simultaneous characterization across different brain areas, i.e., within distributed networks. Here, we conducted a multivariate multimodal analysis in a large and well-characterized ADHD sample through combining gray matter probability, cortical thickness, surface area volume estimates, and white matter diffusion indices.

2. Materials and methods

2.1. Sample

We included 333 participants from the NeuroIMAGE study (www.neuroimage.nl) (von Rhein et al., 2014), the Dutch follow-up of the International Multicenter ADHD Genetics (IMAGE) study (Muller et al., 2011a; Muller et al., 2011b). Participants with ADHD combined type and their siblings (regardless of ADHD diagnosis) were recruited from outpatient

psychiatric or pediatric clinics. Control families were recruited from schools and did not meet criteria for ADHD, neither did their first-degree relatives. Further inclusion criteria in IMAGE were an IQ ≥ 70, European Caucasian descent, and no diagnosis of autism, epilepsy, general learning difficulties, brain disorders, or known genetic disorders (such as Fragile X or Down syndrome). Diagnostic, neurocognitive, MRI, and genetic data for NeuroIMAGE were collected at the VU University Amsterdam and Radboudumc Nijmegen. All participants and their parents (in case of participants below 18 years of age) gave informed consent and the study was approved by local ethical committees. For the current analyses we selected all participants that had both diffusion tensor imaging (DTI) and structural T1 scans of good quality as assessed by visual inspection (n = 333). Participants were divided into two groups based on the presence of an ADHD diagnosis (129 ADHD and 204 non-ADHD; Table 1). There were no differences between the participants included in the current analysis and the complete NeuroIMAGE sample on measures of ADHD severity, age, and gender (p > 0.05).

2.2. Diagnostics

To determine ADHD diagnoses, all participants were assessed using a combination of a semi-structured diagnostic interview and Conners' ADHD questionnaires. Participants were administered the ADHD section of the Schedule for Affective Disorders and Schizophrenia for School-Age Children - Present and Lifetime Version (Kaufman et al., 1997), carried out by trained professionals. Both the parents and the child, if ≥ 12 years old, were interviewed separately and were initially only administered the ADHD screening interview. Participants with elevated scores on any of the screen items were administered the full ADHD section. Further each child was assessed with a teacher-rating (Conners' Teacher Rating Scale - Revised: Long version (CTRS-R:L); (Conners et al., 1998); applied for children <18 years) or a self-report (Conners' Adult ADHD Rating Scales - Self-Report:Long Version (CAARS-S:L); (Conners et al., 1999); applied for children ≥18 years). A diagnostic algorithm was applied to combine symptom counts on the K-SADS and CTRS-R:L (for participants <18 years) or CAARS-S:L (for participants ≥18), providing operational definitions of each of the 18 behavioral symptoms of ADHD defined by the DSM-IV (American Psychiatric Association, 2000). Symptoms of the CTRS-R:L or CAARS-S:L were only used in the algorithm if at least 2 symptoms were reported on this questionnaire. Participants with a combined symptom count of ≥6 symptoms of hyperactive/impulsive behaviour and/or inattentive behaviour were diagnosed with ADHD, provided they: a) met the DSM-IV criteria for pervasiveness and impact of the disorder (measures derived from the K-SADS), b) showed an age of onset before 7, derived from the K-SADS, and c) received a T ≥ 63 on at least one of the DSM ADHD scales on either one of Conners' ADHD questionnaires. Criteria were slightly adapted for young adults (≥18 years), such that a combined symptom count of 5 symptoms was sufficient for a diagnosis (Kooij et al., 2005), also in accordance with the ADHD algorithm in DSM-5. Participants not meeting the criteria for an ADHD diagnosis were assigned to the non-ADHD group. For participants using stimulant medication, participants were asked to fill out the questionnaires keeping a period of time when they were off medication in mind. For the testing day, participants were asked to withhold the use of psychoactive medication for 48 h before visit.

Comorbidity with oppositional defiant disorder (ODD) and conduct disorder (CD) was assessed using the K-SADS. Initially only the screening interview was administered, thereafter participants with elevated scores on any of the screen items were also administered the full section.

2.3. MRI acquisition

MRI scans were acquired at two different locations (Donders Centre for Cognitive Neuroimaging in Nijmegen, The Netherlands and VU

Table 1
Demographic and clinical characteristics.

	ADHD ($n = 129$)		Non-ADHD ($n = 204$)		Test statistic
Demographic					
Age, mean, SD	17.8	3.2	17.3	3.5	$t(331) = -1.378$
Gender, number, % male	90	69.8%	84	41.2%	$X^2(1) = 25.893$[**]
Scan site, number, % in Nijmegen	68	52.7%	97	47.5%	$X^2(1) = 0.843$
Estimated IQ[b], mean, SD	96.9	15.6	103.0	13.1	$t(328) = 3.794$[**]
History of medication use (yes/no), number, % yes[a]	94	84.7%	15	8.6%	$X^2(1) = 166.011$[**]
Clinical					
Hyperactive/impulsive symptoms[c]	5.6	2.4	0.7	1.3	$t(331) = -24.348$[**]
Inattentive symptoms[c]	7.3	1.6	0.9	1.7	$t(331) = -34.624$[**]
Comorbid ODD, number, %	35	27.1%	5	2.5%	$X^2(1) = 45.547$[**]
Comorbid CD, number, %	6	4.7%	0	0%	$X(1) = 8.163$[*]

ODD = oppositional defiant disorder, CD = conduct disorder.

[a] History of stimulant medication use (based on pharmacy reports) is missing for 48 participants.

[b] Estimated IQ based on Wechsler Intelligence Scale for Children or Wechsler Adult Intelligence Scale–III Vocabulary and Block Design. IQ is missing for 2 ADHD cases and 1 non-ADHD.

[c] Symptom count according to the DSM-IV criteria (range from 0 to 9).

[*] $p < 0.01$.

[**] $p < 0.001$.

University Medical Centre in Amsterdam, The Netherlands), using two comparable 1.5 Tesla MRI scanners (Siemens Sonata/Avanto, Erlangen, Germany), identical 8-channel head-coils, and matched scan protocols. For each participant we obtained a high-resolution T1-weighted MPRAGE anatomical scan (176 sagittal slices, TR = 2730 ms, TE = 2.95 ms, TI = 1000 ms, flip angle = 7 deg, GRAPPA 2 acceleration, voxel size = $1.0 \times 1.0 \times 1.0$ mm, field of view = 256 mm). In addition, whole brain diffusion-weighted images were collected (twice refocused PGSE EPI; 60 diffusion-weighted images; b-factor 1000 s/mm2; 5 non-diffusion-weighted images; 60 slices interleaved; TE/TR = 97/8500 ms; GRAPPA-acceleration 2; voxel size $2.0 \times 2.0 \times 2.2$ mm).

2.4. MRI processing

2.4.1. Measures of gray matter structure

2.4.1.1. Cortical thickness and areal expansion. We extracted cortical thickness and areal expansion estimates using Freesurfer v5.3 software (http://surfer.nmr.mgh.harvard.edu/; (Dale et al., 1999; Fischl et al., 1999)). FreeSurfer is a fully automated technique to create a 3D reconstruction of the cortical sheet that uses both intensity and continuity information. Cortical thickness was calculated as the closest distance from the gray/white boundary to the gray/CSF boundary at each vertex on the surface (Fischl & Dale, 2000). Surface area was defined as the relative amount of expansion or compression at each vertex and was estimated by registering each subject's surface to a common atlas space surface. Surface maps were resampled, mapped to a common coordinate system using a non-rigid high-dimensional spherical averaging method to align cortical folding patterns (Fischl et al., 2008). After bringing the Freesurfer data onto the high-resolution average subject surface (fsaverage), data were projected onto the low-resolution template (fsaverage5: 4 mm voxels) for computational reasons. A 10 mm FWHM surface-based smoothing kernel was applied.

2.4.1.2. VBM. Each participant's T1-weigthed scan was normalized to Montreal Neurological Institute (MNI) 152 standard space, bias-field corrected and segmented into gray matter, white matter, and cerebrospinal fluid using the unified procedure of the VBM 8.1 toolbox (http://dbm.neuro.uni-jena.de/vbm/) in SPM8 (http://www.fil.ion.ucl.ac.uk/spm, London, UK) using default settings. This method uses an optimized VBM protocol (Ashburner & Friston, 2000; Good et al., 2001) as well as a model based on Hidden Markov Random Fields developed to optimize the detection of effects (Cuadra et al., 2005). Correction for total brain volume was incorporated in the analysis (modulated analysis). Regional volumes of gray matter, white matter, and CSF were estimated. Morphometric analysis of white-matter, however, is known to be sensitive to misalignments during spatial normalization (Bookstein,

2001; Jones et al., 2005; Smith et al., 2006). Therefore, the VBM analysis focused on the gray matter segmentation only and we used Tract-based Spatial Statistics (TBSS) to assess white matter microstructure (see next paragraph). Gray matter segmented images were modulated to correct for local expansion or contraction. Generally, Jacobian modulated gray matter values are referred to as gray matter volume, while unmodulated images are referred to as gray matter density maps (Eckert et al., 2006). The latter density maps are sensitive to poor registration as they reflect the proportion of gray matter relative to other tissue types within a region. Thus, here, we focus on gray matter volume estimates to investigate gray matter values. Images were smoothed with a 9.4 mm FWHM Gaussian smoothing kernel (sigma = 4 mm). Data were down-sampled from 2 mm to 4 mm isotropic for computational reasons.

2.4.2. Measures of white matter microstructure

DTI images were denoised, realigned, and corrected for residual eddy-current (SPM8) and for artifacts from head and/or cardiac motion using robust tensor modeling (PATCH (Zwiers, 2010)) and for magnetic susceptibility induced distortions (Visser & Zwiers, 2010). Diffusion tensors and derived FA, MD, and MO values were calculated for each voxel (FSL 4.1.7; (Behrens et al., 2003)). FA quantifies anisotropy of diffusion, with higher FA values indicative of larger directed diffusion (Basser et al., 1994). MD measures the overall magnitude of diffusion with higher values indicating stronger diffusion. MO has been less often reported in the DTI literature; nevertheless, it is a valuable addition to FA and MD as it reflects the shape of the diffusion tensor. MO is mathematically orthogonal to FA and ranges from planar (e.g., in regions with crossing fibers) to linear (when one fiber direction dominates).

Using Tract-Based Spatial Statistics (FSL-TBSS), FA volumes were skeletonized (Smith et al., 2006) and nonlinearly registered to the FMRIB-58_FA template (MNI152-space). Subsequently, a group mean FA-image was created to produce a mean skeleton. Finally, each diffusion parameter (FA, MD, MO) of each participant was projected onto the group skeleton, thresholded at FA ≥ 0.2 to exclude peripheral tracts (Smith et al., 2006). To reduce computational complexity, the resolution of the skeleton was reduced from 1 mm to 2 mm isotropic voxel size and renormalized.

2.5. Linked independent component analysis

Linked independent component analysis (linked ICA, (Groves et al., 2011) is a data-driven approach aimed at relating common components across multiple imaging modalities. Linked ICA is based on the general ICA model (Jutten & Herault, 1991; Hyvarinen & Oja, 2000), a technique that given a multivariate set of mixed signals, searches for non-Gaussian sources that provide a new set of statistically independent signals.

While the traditional ICA algorithms perform a matrix factorization, there exist extensions such as tensor ICA (Beckmann & Smith, 2005) which allow for three dimensional factorizations and, thus, are able to deal with input data composed of different modalities. Tensor-ICA, however, cannot directly deal with data modalities that have different dimensionalities, i.e. where the number of observations between modalities change due to differences in, e.g., resampling. By applying separate ICA decompositions on individual data modalities with different dimensions, linked ICA allows to jointly model these complex input data. Importantly, linked ICA constrains all decompositions to be linked through the same shared subject-courses. The data are modeled as multimodal independent components characterizing sources of intersubject variability. Each component has an associated spatial pattern for every modality, and all modalities are linked through a subject loading vector reflecting the typicality of this component for each participant. Further, linked ICA models the component-specific relevance of each modality in each component through a vector of weights that reflects to which extent each modality contributes to a given independent component (Groves et al., 2011). Thereby linked ICA ensures the balancing of information across modalities by taking into account the spatial correlation of each modality (Groves et al., 2012).

Here, we used linked ICA including the six data modalities described above: cortical thickness, areal expansion estimates, VBM gray matter volume, FA, MD, and MO. Given our sample size and based on previous analyses (Groves et al., 2012), we ran the linked ICA model to estimate 50 independent components.

2.6. Statistics

Spatial patterns of the components were converted to *z*-statistics and were thresholded at z = 3. Subsequent analyses aimed at relating subject loadings of a component to differences in clinical variables of interest (i.e., ADHD diagnosis). Scanner site, gender, age (linear and quadratic fit) were regressed out of the subject loading vectors as they were of no primary interest (effects of the regression on the subject loadings are shown in eFig. 1). First, we correlated the component-specific subject loading vectors with inattentive and hyperactive/impulsive symptoms. Using Bonferroni correction for the total of 50 components a threshold of *p* < 0.001 was set. Secondly, for the components with a significant association, we compared the subject loading vectors between the ADHD and non-ADHD groups using a categorical group comparison. To assess statistical significance, independent sample *t*-tests (two-tailed) were used. A threshold of *p* < 0.05/n, with n = the amount of components with a significant association with ADHD symptoms.

3. Results

3.1. General outcome of the linked ICA analysis

Fig. 1 illustrates the normalized weight vectors reflecting the relative contribution of each modality in each independent component. Of the 50 components, we identified 29 as multimodal, i.e., a single modality does not account for more than 50% of the component weight vector (further described in supplementary material). Further inspection of the subject loadings revealed 4 components significantly related to scanner site, 9 related to age, and 12 associated with gender (eTable 1).

3.2. ADHD-related effects

After regressing out scanner site, gender, age, and age^2, two multimodal components (component 18 and 24) were significantly related to ADHD symptoms. The subjects' loadings of component 18 showed a significant relation with hyperactive/impulsive symptoms *t* (332) = −3.370, *p* < 0.001 (Fig. 2), but not with inattentive symptoms when applying Bonferroni correction, *t*(332) = −2.819, *p* = 0.005.

Relative contribution of modalities in each component
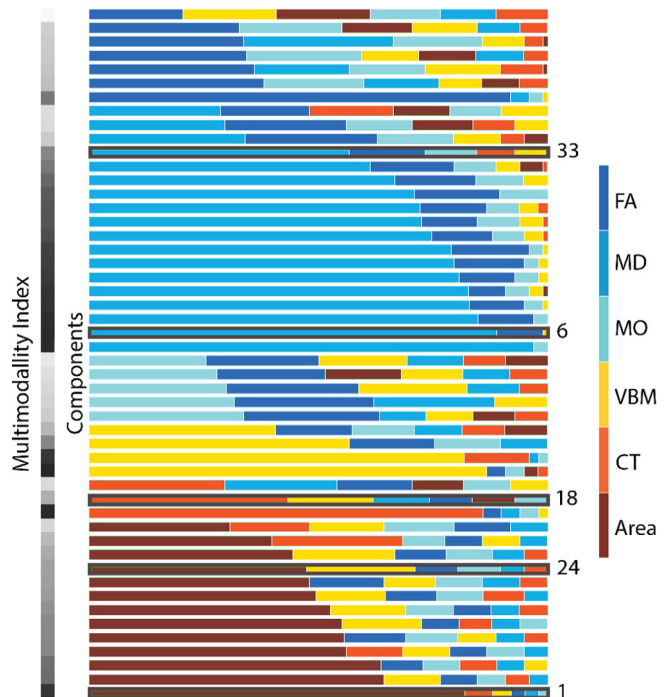
Fig. 1. Relative weight of each modality within each component. Components are sorted first based on the modality that yielded the largest contribution, and second on their level of multimodality, i.e., how evenly distributed several modalities contributed. To quantify multimodality we calculated a multimodal index assigning a value of 1 to components to which each modality contributed equally and 0 to components to which one modality primarily contributed. The multimodal index is plotted in the bar on the left, going from 1 = white, to 0 = black. Components that yielded significant ADHD-related effects are indicated. FA = Fractional Anisotropy, MD = Mean Diffusivity, MO = Diffusion Mode, VBM = Voxel-Based Morphometry, CT = Cortical Thickness Estimate, Area = Areal Expansion Estimate.

Furthermore, ADHD and non-ADHD groups differed significantly from each other in a categorical group comparison *t*(331) = 3.068, *p* = 0.002, with participants with ADHD exhibiting higher scores (M = 0.21, SD = 0.94) compared to non-ADHD participants (M = −0.13, SD = 1.00).

Component 18 had its largest contributions from gray matter volume and cortical thickness data (FA = 9%, MD = 12%, MO = 7%, VBM = 18%, CT = 42%, Area = 9%). Participants with ADHD showed a pattern of lower gray matter volume in the orbitofrontal and anterior cingulate cortex and increased gray matter volume around sensorimotor, occipital, and thalamic regions (Fig. 3). This gray matter volume pattern coincided with decreased cortical thickness in the insula, medial temporal cortices, and precentral gyrus. Although white matter microstructure was contributing less to this component (component 18), the spatial pattern was consistent with the VBM and cortical thickness maps. The DTI maps showed in ADHD, higher FA in the forceps major connecting the occipital lobes, lower FA in the internal capsule containing motor and sensory projection fibers, corpus callosum and around the postcentral cortex, all in conjunction with higher MD in the postcentral cortex and lower MD in the thalamus extending to surrounding structures. Finally, increased MO in the bilateral superior corona radiata was found in ADHD compared to non-ADHD.

Subject loadings on a second multimodal component (component 24) were significantly related to hyperactive/impulsive symptom count *t*(332) = −3.516, *p* < 0.001 (Fig. 4). The association between inattentive symptom count and the subjects' loadings on component 24 did not survive Bonferroni correction, *t*(332) = −2.137, *p* = 0.033. Furthermore, when comparing ADHD and non-ADHD groups directly, participants with ADHD exhibited significantly lower scores (M = −0.18,
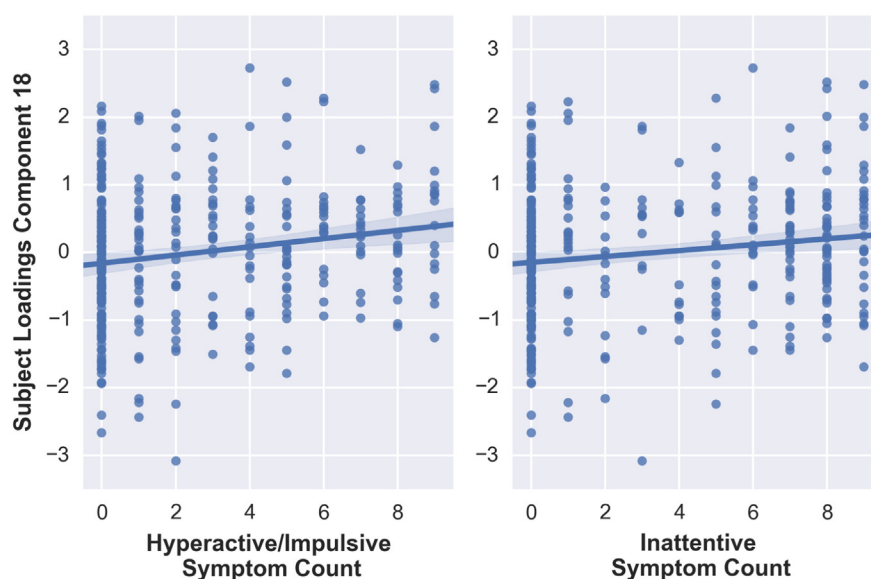
Fig. 2. Correlations between subjects' loadings on component 18 and hyperactive/impulsive and inattentive symptoms counts.

SD = 0.99) compared to non-ADHD participants (M = 0.11, SD = 0.98), $t(331) = 2.660$, $p = 0.008$.

Gray matter volume and areal expansion estimates both encompassed the medial frontal cortex, with larger volumes in non-ADHD participants compared to participants with ADHD (Fig. 5). While the VBM spatial map covered the complete prefrontal lobe, thalamus, and part of cerebellum, the areal expansion estimates map was localized to anterior prefrontal cortex. The contribution of the DTI modalities was smaller (FA = 9%, MD = 5%, MO = 9%, VBM = 23%, CT = 5%, Area = 46%), but consistently showed abnormalities of the prefrontal white matter to be associated with ADHD. Specifically, in ADHD, lower FA was found in the forceps minor combined with lower MO, and lower FA was combined with higher MO in more posterior regions of the forceps minor and superior corona radiata, as well as thalamic and cerebellar regions. Finally, higher MD in the corpus callosum was present in ADHD.

Finally, differences between ADHD and non-ADHD groups on three unimodal components (component 1, 6, and 33) did not survive correction for multiple comparisons. These unimodal components are specified in the supplementary material.

Post-hoc control and sensitivity analyses showed that neither component 18 nor 24 were associated with medication history or IQ. As history of medication use was only relevant for the ADHD group and IQ might reflect variation that is a feature of ADHD pathology itself (Nigg, 2001; Dennis et al., 2009), these variables were not entered in the model, but post-hoc analyzed. Furthermore, adding oppositional defiant disorder/conduct disorder comorbidity to our analyses did not influence the results, and results were similar in a subsample without comorbidities. No interactions between diagnosis and gender were found. Figures illustrating the post-hoc sensitivity analyses are presented in the supplementary material.

3.3. Multimodal versus unimodal findings

To investigate the added value of our multimodal analysis over a unimodal analysis, we compared current multimodal results with previously published unimodal results obtained from the same cohort. Results of three modalities were reported recently, namely: VBM gray matter volume estimates (Bralten et al., under review), cortical thickness (Schweren et al., 2015), and DTI (van Ewijk et al., 2014).

In a VBM study, we reported smaller gray matter volumes in five clusters in the precentral gyrus, medial and orbital frontal cortex, frontal pole and (para)cingulate cortex (Bralten et al., under review). Indeed, prefrontal regions were also revealed by the present multimodal analysis (see eFig. 6 for spatial overlap). When comparing the contribution of VBM data to components 18 and 24, we see that component 24 had the largest contribution of VBM data (23% compared to 18%). In addition, the spatial pattern of component 24 also showed the largest overlap with the unimodal results. This indicates that the modality with the largest contribution also replicates the unimodal results the most consistently. Furthermore, clusters revealed by the multimodal analysis were larger and more symmetrical, indicating increased sensitivity to ADHD related effects by the joint analysis of all modalities. Note that patterns appearing to be symmetric are not a trivial finding since the algorithm used imposes no spatial structure. In addition, the multimodal analysis revealed that these ADHD-related alterations in gray matter volume co-occurred with changes in areal expansion and white matter indices. Importantly, by using a multimodal analysis method where individual decompositions are linked together by means of a subject-loading vector, one can be confident that the same subjects are driving the patterns present in different modalities. This is fundamentally different from unimodal analyses where the actual association between subject specific values across modalities needs to be established post-hoc. Thus, the multimodal analysis does not only replicate the unimodal VBM findings; in addition, it reveals a consistent pattern of prefrontal abnormalities in areal expansion estimates, FA and MO (see Fig. 5) in the same subjects.

For the unimodal cortical thickness data analysis, we reported thinner bilateral medial temporal cortices in ADHD, including in the entorhinal, parahippocampal, fusiform and isthmus cingulate cortices (Schweren et al., 2015). Parts of the temporal cortex also showed decreased cortical thickness in multimodal component 18 (see eFig. 7 for spatial overlap). Cortical thickness estimates had the largest contribution to this component. Nevertheless, by including other modalities the involvement of frontal gray matter volume was revealed, indicating the role of the more extended fronto-limbic system in ADHD pathology.

Finally, in a previous DTI study, we reported widespread differences in white matter indices (FA and MD) between ADHD and control groups (van Ewijk et al., 2014). When visually inspecting the multimodal components that were related to ADHD (component 18 and 24), overlap with unimodal findings was limited (eFig. 8). This is not surprising as the contribution of the diffusion indices to these components was limited (see Fig. 1). Furthermore, when inspecting the components that were related to ADHD but did not show a significant multimodal
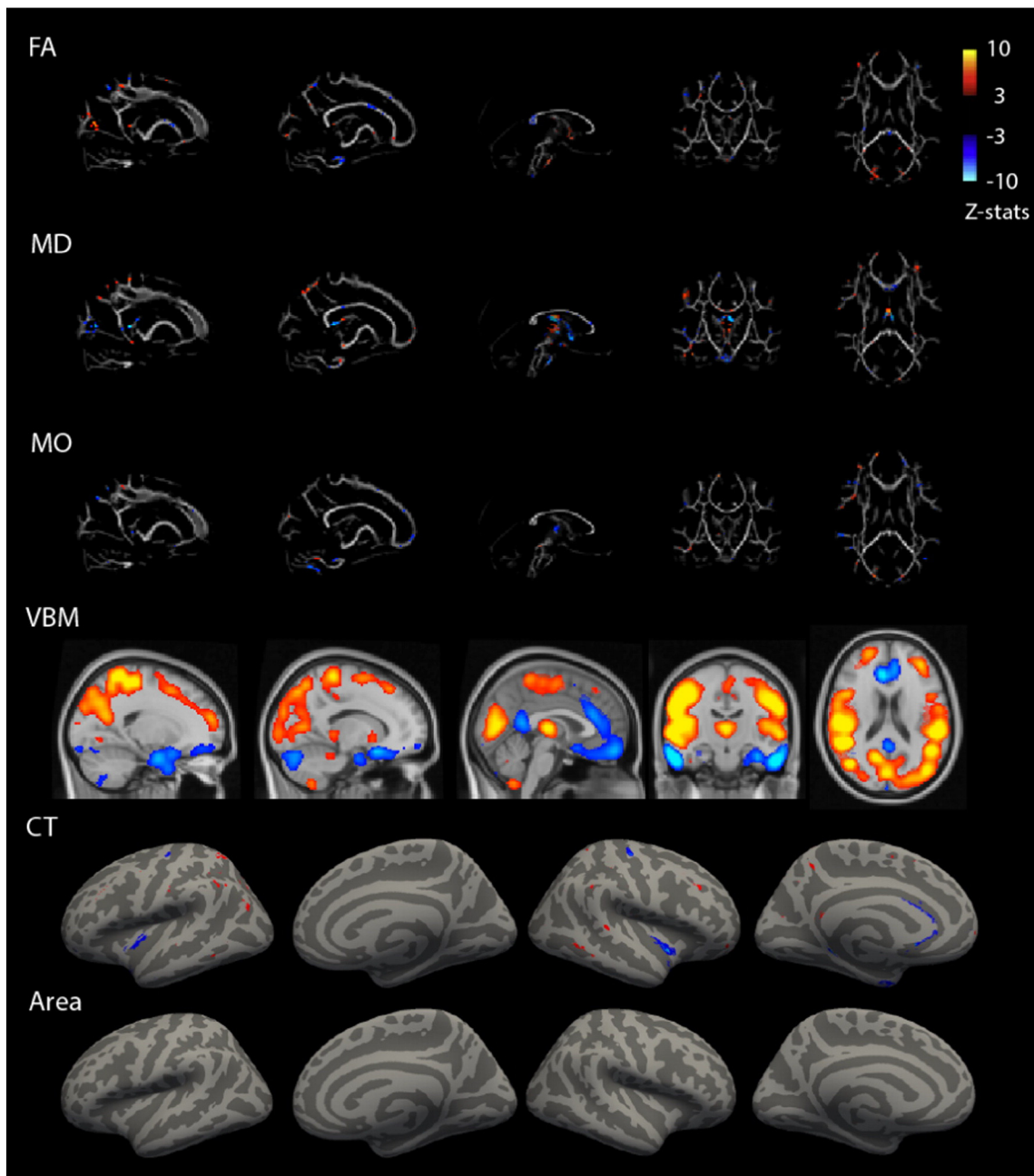
Fig. 3. Multimodal component 18 related to ADHD. Spatial representation of each modality's contribution to component 18. Spatial maps were thresholded at z = 3. Blue colors indicate lower values on this MRI measure for ADHD than for control. VBM = Voxel-Based Morphometry gray matter volume, FA = Fractional Anisotropy, MD = Mean Diffusivity, MO = Diffusion Mode.

character (component 1, 6, and 33), MD of component 6 showed high overlap with previously published unimodal MD results (van Ewijk et al., 2014) (eFig. 9). The spatial maps encompass the corpus callosum, internal capsule, posterior thalamic radiation, corona radiata, fornix, cerebellar peduncle, and cingulum. Further, spatial maps of unimodal FA analysis (van Ewijk et al., 2014) were partly reflected in component 39 (eFigs. 10 and 11). Although this component was not significantly different between ADHD and non-ADHD groups, [$t(331) = 1.929$, $p = 0.055$], it was significantly related to the subjects' K-GAS score [$t(332) = 3.166$, $p = 0.002$]. This K-GAS score reflects the general functioning of participants and was highly correlated with the inattentive ($r = -0.75$) and hyperactive/impulsive symptom count ($r = -0.67$). Finally, DTI findings of the multimodal components (component 18 and 24) were explaining variance that was also reflected in other modalities and spatially consistent across modalities. While prefrontal

white matter was not revealed by the unimodal analysis, our multimodal analysis picked up on variation in prefrontal white matter which was also observable in prefrontal gray matter volume (see Fig. 5).

4. Discussion

Imaging studies in neuropsychiatry typically focus on single imaging modalities such as brain volume or white matter microstructure. Here, we aimed to uncover shared pathophysiological processes in gray and white matter using a multivariate analysis technique that allows investigating concurrent patterns of variation in the brain across modalities (Groves et al., 2011). Including data on various aspects of brain morphology and white matter microstructure, we identified modality transcending differences between participants with and without
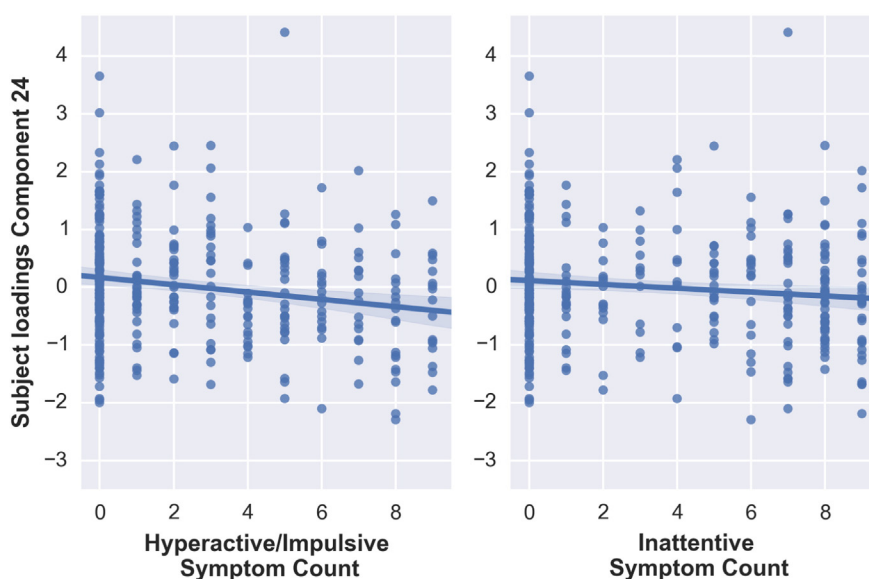
Fig. 4. Correlations between subjects' loadings on component 24 and hyperactive/impulsive and inattentive symptoms counts.

ADHD in fronto-striatal and fronto-limbic circuits, as well as in parietal and occipital lobes, insula, and cerebellum.

We observed reduced prefrontal gray matter volume and surface area in participants with ADHD compared to those without ADHD, thereby confirming previous studies (Narr et al., 2009; Shaw et al., 2012; Overmeyer et al., 2001; Seidman et al., 2005; Almeida et al., 2010; Batty et al., 2010; Durston et al., 2005). In addition, and again in line with previous studies, we observed abnormal microstructure of prefrontal white matter (van Ewijk et al., 2012; Pavuluri et al., 2009; Konrad & Eickhoff, 2010). The prefrontal cortex is of clear interest in ADHD research, as it underlies performance on executive functioning tasks that are impaired in ADHD (Barkley, 1997; Willcutt et al., 2005). Next to prefrontal gray matter, prefrontal white matter microstructure has been associated with poor executive functioning in ADHD (Lawrence et al., 2013). As the prefrontal cortex is part of fronto-striatal and fronto-cerebellar loops (Alexander et al., 1986), striatal and cerebellar regions may be expected to show concurrent changes. Indeed, we observed abnormal volumes of thalamus and cerebellum in ADHD. Our results indicate that the entire fronto-striatal loops (i.e., both white and gray matter) are affected in ADHD, supporting the idea that the pathophysiology of ADHD is reflected across large-scale networks, rather than confined to specific areas within the brain (Menon, 2011).

We also observed decreased gray matter volume in the orbitofrontal cortex, ACC, and insula in ADHD. These fronto-limbic regions have been reported as altered in previous unimodal studies in ADHD and have been related to abnormal reinforcement responses, error monitoring, and emotional processing (Frodl & Skokauskas, 2012; Amico et al., 2011; Hesslinger et al., 2002; Proal et al., 2011; Hoekzema et al., 2012). Related to the same underlying between-participant variance as the fronto-limbic regions, more basal sensory areas, i.e., occipital and sensori-motor cortex were included in this ADHD-related component. These areas are implicated in, respectively, attention and motor performance. In line with previous reports, we observed increased volume of the regions in ADHD compared to non-ADHD participants (van Wingen et al., 2013; Wang et al., 2007). When comparing our results with the literature, it has to be noted that our non-ADHD group contains a wider spectrum of ADHD characteristics than is commonly included in a control group. In light of the dimensional analyses this allows the modeling of the entire ADHD spectrum.

Using a multimodal approach, we replicated our previously published unimodal findings in the same cohort. Specifically, gray matter

volume and cortical thickness results showed high overlap between unimodal and multimodal analyses. An integrated multimodal method often reveals findings in one modality that could also have been revealed using a unimodal method. However, a unimodal analysis per definition overlooks part of the picture as it is focusing only on this one modality. Here, we show that the addition of more modalities reveals that unimodal findings can be reflected across modalities, e.g., co-occurring abnormalities in prefrontal gray matter volume, prefrontal FA, and prefrontal areal expansion estimates. Furthermore, when conducting multiple unimodal analyses no conclusions can be drawn about the individual subjects that drive the effects in different modalities, therefore the modalities then need to be reconsolidated post-hoc. In addition, the multimodal maps showed more extended and symmetric spatial maps than the unimodal results, indicating increased sensitivity by adding modalities to the analysis. Power in a unimodal analysis is dependent on the signal-to-noise (SNR) properties of that specific modality. Importantly, in a multimodal analysis SNRs of each modality are linked. As a consequence, power in modalities with lower SNR is enhanced by exploiting statistical regularities existing at the population level. In the case of linked ICA, these regularities resemble subject loadings across subjects (Groves et al., 2012). Moreover, using the multimodal approach we observe that unimodal findings were replicated in the modality that had the largest contribution to this component and thus, that unimodal findings were reflected in spatial maps of different multimodal components, e.g., gray matter volume data in component 24 and cortical thickness results in component 18. Concerning the DTI findings, unimodal MD findings were reflected in a component that was related to ADHD, but was not multimodal (component 6). While the variance in MD captured by this component was not related to variance in other modalities, the multimodal approach was still able to extract it. Unimodal FA results were partly replicated in component 39, a component that was related to the general functioning in daily life of the participants.

Although the linked ICA approach employed here does not reveal new pathophysiology related to ADHD, it advances on classic unimodal analyses in several ways. Firstly, by modeling the multimodal data within one model linked by the single subject-loading vector, one can be sure that the patterns reflected in different modalities are driven by the same participants. Importantly, this conclusion cannot be reached when conducting parallel unimodal analyses. The knowledge that the same participants show a similar pattern across brain measures, does not only add to the complete image of ADHD, but also opens possibilities
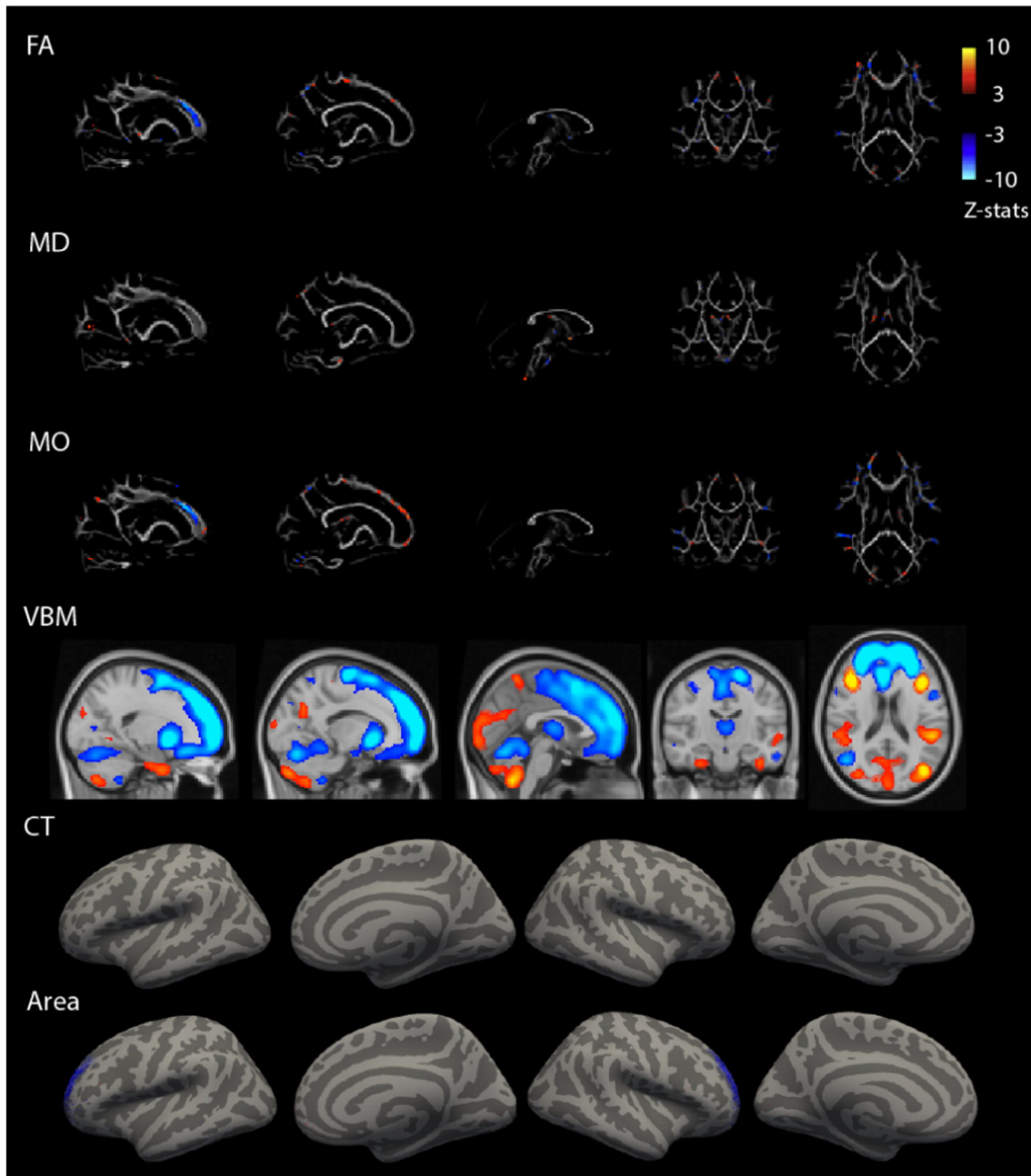
Fig. 5. Multimodal component 24 related to ADHD. Spatial representation of each modality's contribution to component 24. Spatial maps were thresholded at z = 3. Blue colors indicate lower values on this MRI measure for ADHD than control. VBM = Voxel-Based Morphometry gray matter volume, FA = Fractional Anisotropy, MD = Mean Diffusivity, MO = Diffusion Mode.

for more elaborate ways of stratification or subtyping of participants with ADHD based on different brain patterns across MRI modalities. Secondly, as linked ICA allows the inclusion of multiple modalities, shared variance across modalities is modeled, thereby increasing sensitivity to between-participant effects: large unimodal effects will be detected both by unimodal and multimodal analyses. Small effects that are present in several modalities, however, might only be revealed when variance present across modalities is adequately modeled, increasing the sensitivity to effects that have small individual unimodal effect sizes but consistent across the population and across modalities. Finally, structural variation within the data related to nuisance variables is captured within separate components. As an example, we observed components that were dominated by scan site or gender, thereby capturing main sources of variance of no-interest within our dataset. As such, linked ICA has the potential to address common imbalances in

gender and/or age present in many clinical samples. Of note, in order to remove any residual variance not captured within these independent components, we additionally regressed scan site, gender, and age out of the data.

Under the multimodal model, the cause of convergence of between-participant variability across modalities may be a common pathophysiologic process that is reflected in all modalities. Such processes could be related to common etiologic factors, either genetic or environmental, or both. Such etiologic factors might already exert their influence during prenatal development (Sidman & Rakic, 1973), influencing proliferation and migration of cells. As such, genetic factors that are associated with the development of brain structure have suggested to be implicated in ADHD. One example are polymorphisms within genes related to neurodevelopmental processes such as cell adhesion, neuron migration, and neurite outgrowth (Poelmans et al., 2011; Yang et al., 2013).

Likewise, environmental factors have been shown to exert influence on brain development, e.g., the influence of maternal smoking on brain development (Roza et al., 2007).

Instead of a common etiologic factor simultaneously affecting modalities, it is also possible that a cascade of sequential events results in effects across modalities. In this case, the pathophysiologic process primarily affects one modality, in turn leading to alterations in other modalities. This has been hypothesized in Alzheimer's disease research, where gray matter atrophy is thought to lead to disruptions in white matter tracts (Villain et al., 2010). The identification of the starting event could then significantly advance possibilities for preventive or therapeutic interventions. Yet, outlining such cascading model in developmental psychiatric disorders is obscured by the early onset of the disorder and a manifold of potentially interacting neurobiological and social-environmental processes. Prospective brain imaging studies in high-risk young children may provide helpful insights in this context through improved longitudinal modeling of developmental brain processes.

Interpretation of multimodal analyses will greatly benefit from improved knowledge concerning the underlying developmental trajectories of different modalities, which is currently limited to rather general descriptions. As an example, developmental changes in white matter follow a linear pattern, while development of the cortex follows an inverted U-shape pattern across development (Gogtay et al., 2004; Paus et al., 1999). Furthermore, developmental processes of different modalities might interact. For instance, increased myelination of intracortical fibers and synaptic pruning might induce an apparent loss of cortex and account for the cortical thinning observed during puberty (Gogtay et al., 2004; Paus, 2005). In the absence of longitudinal multimodal investigations, little is known about potentially common underlying processes and developmental trajectories.

In conclusion, our results advance prior studies by providing evidence that distinct structural properties of multiple brain areas are simultaneously affected in ADHD. In line with previous literature, we observed ADHD-related changes in prefrontal cortex, as well as parietal, insular, and occipital areas. We showed that these structural changes were reflected by multimodal components that capture commonalities across participants. Such reflection of ADHD-pathology across structural brain modalities offers a biologically meaningful characterization of ADHD by suggesting common pathophysiological processes without the need for post-hoc cross-modal meta-analysis. This paves the way for further research into the functional significance of these multimodal components for neurocognitive performance, neural activation to cognitive tasks, and treatment response patterns and into brain-based stratification of participants with ADHD.

Potential conflicts of interest

Jan K Buitelaar has been in the past 3 years a consultant to/member of advisory board of/and/or speaker for Janssen Cilag BV, Eli Lilly, Shire, Lundbeck, Roche and Servier. He is not an employee of any of these companies, and not a stock shareholder of any of these companies. He has no other financial or material support, including expert testimony, patents, and royalties.

Jaap Oosterlaan has been on the advisory board of Shire and UCB Pharmaceuticals. He has received an unrestricted grant from Shire.

Pieter Hoekstra has received honoraria for advice from Eli Lilly and Shire.

In the past year, Dr. Faraone received income, travel expenses, potential income and/or research support from Pfizer, Ironshore, Shire, Akili Interactive Labs, CogCubed, Alcobra, VAYA Pharma, Neurovance, Impax, NeuroLifeSciences. With his institution, he has US patent US20130217707 A1 for the use of sodium-hydrogen exchange inhibitors in the treatment of ADHD. He receives royalties from books published by Guilford Press: Straight Talk about Your Child's Mental Health, Oxford University Press: Schizophrenia: The Facts and Elsevier, ADHD: Non-Pharmacologic Interventions.

Christian F. Beckmann receives consulting income from and is shareholder of SBGneuro Ltd.

Barbara Franke received a speaker fee from Merck.

The other authors have no potentially competing interests.

Acknowledgements

Appendix A. Supplementary data

Supplementary data to this article can be found online at http://dx.doi.org/10.1016/j.nicl.2016.03.005.

References

Groves, A.R., Beckmann, C.F., Smith, S.M., Woolrich, M.W., 2011. Linked independent component analysis for multimodal data fusion. NeuroImage 54 (3), 2198–2217. http://dx.doi.org/10.1016/j.neuroimage.2010.09.073 (PubMed PMID: 20932919).

Castellanos, F.X., Lee, P.P., Sharp, W., Jeffries, N.O., Greenstein, D.K., Clasen, L.S., et al., 2002. Developmental trajectories of brain volume abnormalities in children and adolescents with attention-deficit/hyperactivity disorder. J. Am. Med. Assoc. 288 (14), 1740–1748 (PubMed PMID: 12365958).

Narr, K.L., Woods, R.P., Lin, J., Kim, J., Phillips, O.R., Del'Homme, M., et al., 2009. Widespread cortical thinning is a robust anatomical marker for attention-deficit/hyperactivity disorder. J. Am. Acad. Child Adolesc. Psychiatry 48 (10), 1014–1022. http://dx.doi.org/10.1097/CHI.0b013e3181b395c0 (PubMed PMID: 19730275; PubMed Central PMCID: PMC2891193).

Shaw, P., Eckstrand, K., Sharp, W., Blumenthal, J., Lerch, J.P., Greenstein, D., et al., 2007. Attention-deficit/hyperactivity disorder is characterized by a delay in cortical maturation. Proc. Natl. Acad. Sci. U. S. A. 104 (49), 19649–19654. http://dx.doi.org/10.1073/pnas.0707741104 (PubMed PMID: 18024590; PubMed Central PMCID: PMC2148343).

Shaw, P., Malek, M., Watson, B., Sharp, W., Evans, A., Greenstein, D., 2012. Development of cortical surface area and gyrification in attention-deficit/hyperactivity disorder. Biol. Psychiatry 72 (3), 191–197. http://dx.doi.org/10.1016/j.biopsych.2012.01.031 (PubMed PMID: 22418014).

Greven, C.U., Bralten, J., Mennes, M., O'Dwyer, L., van Hulzen, K.J., Rommelse, N., et al., 2015. Developmentally stable whole-brain volume reductions and developmentally sensitive caudate and putamen volume alterations in those with attention-deficit/hyperactivity disorder and their unaffected siblings. JAMA Psychiatry. http://dx.doi.org/10.1001/jamapsychiatry.2014.3162 (PubMed PMID: 25785435).

Frodl, T., Skokauskas, N., 2012. Meta-analysis of structural MRI studies in children and adults with attention deficit hyperactivity disorder indicates treatment effects. Acta

Psychiatr. Scand. 125 (2), 114–126. http://dx.doi.org/10.1111/j.1600-0447.2011.01786.x (PubMed PMID: 22118249).

Plessen, K.J., Bansal, R., Zhu, H., Whiteman, R., Amat, J., Quackenbush, G.A., et al., 2006. Hippocampus and amygdala morphology in attention-deficit/hyperactivity disorder. Arch. Gen. Psychiatry 63 (7), 795–807. http://dx.doi.org/10.1001/archpsyc.63.7.795 (PubMed PMID: 16818869; PubMed Central PMCID: PMC2367150).

Mackie, S., Shaw, P., Lenroot, R., Pierson, R., Greenstein, D.K., Nugent 3rd, T.F., et al., 2007. Cerebellar development and clinical outcome in attention deficit hyperactivity disorder. Am. J. Psychiatry 164 (4), 647–655. http://dx.doi.org/10.1176/appi.ajp.164.4.647 (PubMed PMID: 17403979).

Nakao, T., Radua, J., Rubia, K., Mataix-Cols, D., 2011. Gray matter volume abnormalities in ADHD: voxel-based meta-analysis exploring the effects of age and stimulant medication. Am. J. Psychiatry 168 (11), 1154–1163. http://dx.doi.org/10.1176/appi.ajp.2011.11020281 (PubMed PMID: 21865529).

van Ewijk H, Heslenfeld DJ, Zwiers MP, Buitelaar JK, Oosterlaan J. Diffusion tensor imaging in attention deficit/hyperactivity disorder: a systematic review and meta-analysis. Neurosci. Biobehav. Rev. 2012;36(4):1093–106. Epub 2012/02/07. http://dx.doi.org/10.1016/j.neubiorev.2012.01.003S0149-7634(12)00010-3 [pii]. (PubMed PMID: 22305957).

Groves, A.R., Smith, S.M., Fjell, A.M., Tamnes, C.K., Walhovd, K.B., Douaud, G., et al., 2012. Benefits of multi-modal fusion analysis on a large-scale dataset: life-span patterns of inter-subject variability in cortical morphometry and white matter microstructure. NeuroImage 63 (1), 365–380. http://dx.doi.org/10.1016/j.neuroimage.2012.06.038 (PubMed PMID: 22750721).

von Rhein, D., Mennes, M., van Ewijk, H., Groenman, A.P., Zwiers, M.P., Oosterlaan, J., et al., 2014. The NeuroIMAGE study: a prospective phenotypic, cognitive, genetic and MRI study in children with attention-deficit/hyperactivity disorder. Design and descriptives. Eur. Child Adolesc. Psychiatry. http://dx.doi.org/10.1007/s00787-014-0573-4 Epub 2014/07/12. (PubMed PMID: 25012461).

Muller UC, Asherson P, Banaschewski T, Buitelaar JK, Ebstein RP, Eisenberg J, et al. The impact of study design and diagnostic approach in a large multi-centre ADHD study. Part 1: ADHD symptom patterns. BMC Psychiatry. 2011a;11:54. http://dx.doi.org/10.1186/1471-244X-11-541471-244X-11-54 [pii]. (Epub 2011/04/09. PubMed PMID: 21473745; PubMed Central PMCID: PMC3082291).

Muller UC, Asherson P, Banaschewski T, Buitelaar JK, Ebstein RP, Eisenberg J, et al. The impact of study design and diagnostic approach in a large multi-centre ADHD study: part 2: dimensional measures of psychopathology and intelligence. BMC Psychiatry. 2011b;11:55. http://dx.doi.org/10.1186/1471-244X-11-551471-244X-11-55 [pii]. (Epub 2011/04/09. PubMed PMID: 21473746; PubMed Central PMCID: PMC3090338).

Kaufman, J., Birmaher, B., Brent, D., Rao, U., Flynn, C., Moreci, P., et al., 1997. Schedule for affective disorders and schizophrenia for school-age children-present and lifetime version (K-SADS-PL): initial reliability and validity data. J. Am. Acad. Child Adolesc. Psychiatry 36 (7), 980–988. http://dx.doi.org/10.1097/00004583-199707000-00021 (S0890-8567(09)62555-7 [pii]; Epub 1997/07/01. PubMed PMID: 9204677).

Conners, C.K., Sitarenios, G., Parker, J.D.A., Epstein, J.N., 1998. Revision and restandardization of the conners teacher rating scale (CTRS-R): factor structure, reliability, and criterion validity. J. Abnorm. Child Psychol. 26 (4), 279–291.

Conners, C.K., Erhardt, D., Sparrow, E.P., 1999. Conner's Adult ADHD Rating Scales: CAARS: Multi-Health Systems. North Tonawanda, NY.

American Psychiatric Association, 2000. Diagnostic and Statistical Manual of Mental Disorders: DSM-IV-TR. American Psychiatric Publishing, Inc.

Kooij, S.J.J., Buitelaar, J.K., van den Oord, E.J., Furer, J.W., Th Rijnders, C.A., Hodiamont, P.P.G., 2005. Internal and external validity of attention-deficit hyperactivity disorder in a population-based sample of adults. Psychol. Med. 35 (06), 817–827.

Dale, A.M., Fischl, B., Sereno, M.I., 1999. Cortical surface-based analysis. I. Segmentation and surface reconstruction. NeuroImage 9 (2), 179–194. http://dx.doi.org/10.1006/nimg.1998.0395 (PubMed PMID: 9931268).

Fischl, B., Sereno, M.I., Dale, A.M., 1999. Cortical surface-based analysis. II: inflation, flattening, and a surface-based coordinate system. NeuroImage 9 (2), 195–207. http://dx.doi.org/10.1006/nimg.1998.0396 (PubMed PMID: 9931269).

Fischl, B., Dale, A.M., 2000. Measuring the thickness of the human cerebral cortex from magnetic resonance images. Proc. Natl. Acad. Sci. U. S. A. 97 (20), 11050–11055. http://dx.doi.org/10.1073/pnas.200033797 (PubMed PMID: 10984517; PubMed Central PMCID: PMC27146).

Fischl, B., Rajendran, N., Busa, E., Augustinack, J., Hinds, O., Yeo, B.T., et al., 2008. Cortical folding patterns and predicting cytoarchitecture. Cereb. Cortex 18 (8), 1973–1980. http://dx.doi.org/10.1093/cercor/bhm225 (PubMed PMID: 18079129; PubMed Central PMCID: PMC2474454).

Ashburner J, Friston KJ. Voxel-based morphometry — the methods. NeuroImage. 2000;11 (6):805–21. http://dx.doi.org/10.1006/nimg.2000.0582. (PubMed PMID: ISI: 000087963600018).

Good CD, Johnsrude IS, Ashburner J, Henson RNA, Friston KJ, Frackowiak RSJ. A voxel-based morphometric study of ageing in 465 normal adult human brains. NeuroImage. 2001;14(1):21–36. http://dx.doi.org/10.1006/nimg.2001.0786. (PubMed PMID: ISI: 000169498000003).

Cuadra MB, Cammoun L, Butz T, Cuisenaire O, Thiran JP. Comparison and validation of tissue modelization and statistical classification methods in T1-weighted MR brain images. IEEE Trans. Med. Imaging. 2005;24(12):1548–65. http://dx.doi.org/10.1109/Tmi.2005.857652. (PubMed PMID: ISI:000233779000003).

Bookstein, F.L., 2001. "Voxel-based morphometry" should not be used with imperfectly registered images. NeuroImage 14 (6), 1454–1462. http://dx.doi.org/10.1006/nimg.2001.0770 (PubMed PMID: 11707101).

Jones, D.K., Symms, M.R., Cercignani, M., Howard, R.J., 2005. The effect of filter size on VBM analyses of DT-MRI data. NeuroImage 26 (2), 546–554. http://dx.doi.org/10.1016/j.neuroimage.2005.02.013 (PubMed PMID: 15907311).

Smith, S.M., Jenkinson, M., Johansen-Berg, H., Rueckert, D., Nichols, T.E., Mackay, C.E., et al., 2006. Tract-based spatial statistics: voxelwise analysis of multi-subject diffusion data. NeuroImage 31 (4), 1487–1505. http://dx.doi.org/10.1016/j.neuroimage.2006.02.024 (PubMed PMID: 16624579).

Eckert, M.A., Tenforde, A., Galaburda, A.M., Bellugi, U., Korenberg, J.R., Mills, D., et al., 2006. To modulate or not to modulate: differing results in uniquely shaped Williams syndrome brains. NeuroImage 32 (3), 1001–1007. http://dx.doi.org/10.1016/j.neuroimage.2006.05.014 (PubMed PMID: 16806978).

Zwiers MP. Patching cardiac and head motion artefacts in diffusion-weighted images. NeuroImage 2010;53(2):565–75. Epub 2010/07/06. http://dx.doi.org/10.1016/j.neuroimage.2010.06.014S1053-8119(10)00858-X [pii]. (PubMed PMID: 20600997).

Visser, E.Q.S., Zwiers, J., 2010. EPI Distortion Correction by Constrained Nonlinear Coregistration Improves Group fMRI. Joint Annual Meeting ISMRM-ESMRMB, Stockholm, Sweden.

Behrens, T.E., Woolrich, M.W., Jenkinson, M., Johansen-Berg, H., Nunes, R.G., Clare, S., et al., 2003. Characterization and propagation of uncertainty in diffusion-weighted MR imaging. Magn. Reson. Med. 50 (5), 1077–1088. http://dx.doi.org/10.1002/mrm.10609 (Epub 2003/10/31. PubMed PMID: 14587019).

Basser, P.J., Mattiello, J., LeBihan, D., 1994. MR diffusion tensor spectroscopy and imaging. Biophys. J. 66 (1), 259–267. http://dx.doi.org/10.1016/S0006-3495(94)80775-1 (S0006-3495(94)80775-1 [pii]; Epub 1994/01/01. PubMed PMID: 8130344; PubMed Central PMCID: PMC1275686).

Jutten C, Herault J. Blind separation of sources. 1. An adaptive algorithm based on neuromimetic architecture. Signal Process. 1991;24(1):1–10. doi: Doi 10.1016/0165-1684(91)90079-X. (PubMed PMID: WOS:A1991FZ33700001).

Hyvarinen, A., Oja, E., 2000. Independent component analysis: algorithms and applications. Neural Networks: The Official Journal of the International Neural Network Society 13 (4–5), 411–430 (PubMed PMID: 10946390).

Beckmann, C.F., Smith, S.M., 2005. Tensorial extensions of independent component analysis for multisubject FMRI analysis. NeuroImage 25 (1), 294–311. http://dx.doi.org/10.1016/j.neuroimage.2004.10.043 (PubMed PMID: 15734364).

Nigg, J.T., 2001. Is ADHD a disinhibitory disorder? Psychol. Bull. 127 (5), 571–598 (Epub 2001/09/11. PubMed PMID: 11548968).

Dennis, M., Francis, D.J., Cirino, P.T., Schachar, R., Barnes, M.A., Fletcher, J.M., 2009. Why IQ is not a covariate in cognitive studies of neurodevelopmental disorders. J. Int. Neuropsychol. Soc. 15 (3), 331–343. http://dx.doi.org/10.1017/S1355617709090481 (PubMed PMID: 19402919; PubMed Central PMCID: PMC3075072).

Schweren, L.J., Hartman, C.A., Heslenfeld, D.J., van der Meer, D., Franke, B., Oosterlaan, J., et al., 2015. Thinner medial temporal cortex in adolescents with attention-deficit/hyperactivity disorder and the effects of stimulants. J. Am. Acad. Child Adolesc. Psychiatry 54 (8), 660–667. http://dx.doi.org/10.1016/j.jaac.2015.05.014 (PubMed PMID: 26210335).

van Ewijk, H., Heslenfeld, D.J., Zwiers, M.P., Faraone, S.V., Luman, M., Hartman, C.A., et al., 2014. Different mechanisms of white matter abnormalities in attention-deficit/hyperactivity disorder: a diffusion tensor imaging study. J. Am. Acad. Child Adolesc. Psychiatry 53 (7), 790–799. http://dx.doi.org/10.1016/j.jaac.2014.05.001 (e3; PubMed PMID: 24954828).

Overmeyer, S., Bullmore, E.T., Suckling, J., Simmons, A., Williams, S.C., Santosh, P.J., et al., 2001. Distributed grey and white matter deficits in hyperkinetic disorder: MRI evidence for anatomical abnormality in an attentional network. Psychol. Med. 31 (8), 1425–1435 (PubMed PMID: 11722157).

Seidman, L.J., Valera, E.M., Makris, N., 2005. Structural brain imaging of attention-deficit/hyperactivity disorder. Biol. Psychiatry 57 (11), 1263–1272. http://dx.doi.org/10.1016/j.biopsych.2004.11.019 (PubMed PMID: 15949998).

Almeida, L.G., Ricardo-Garcell, J., Prado, H., Barajas, L., Fernandez-Bouzas, A., Avila, D., et al., 2010. Reduced right frontal cortical thickness in children, adolescents and adults with ADHD and its correlation to clinical variables: a cross-sectional study. J. Psychiatr. Res. 44 (16), 1214–1223. http://dx.doi.org/10.1016/j.jpsychires.2010.04.026 (PubMed PMID: 20510424).

Batty, M.J., Liddle, E.B., Pitiot, A., Toro, R., Groom, M.J., Scerif, G., et al., 2010. Cortical gray matter in attention-deficit/hyperactivity disorder: a structural magnetic resonance imaging study. J. Am. Acad. Child Adolesc. Psychiatry 49 (3), 229–238 (PubMed PMID: 20410712; PubMed Central PMCID: PMC2829134).

Durston, S., Fossella, J.A., Casey, B.J., Hulshoff Pol, H.E., Galvan, A., Schnack, H.G., et al., 2005. Differential effects of DRD4 and DAT1 genotype on fronto-striatal gray matter volumes in a sample of subjects with attention deficit hyperactivity disorder, their unaffected siblings, and controls. Mol. Psychiatry 10 (7), 678–685. http://dx.doi.org/10.1038/sj.mp.4001649 (PubMed PMID: 15724142).

Pavuluri, M.N., Yang, S., Kamineni, K., Passarotti, A.M., Srinivasan, G., Harral, E.M., et al., 2009. Diffusion tensor imaging study of white matter fiber tracts in pediatric bipolar disorder and attention-deficit/hyperactivity disorder. Biol. Psychiatry 65 (7), 586–593. http://dx.doi.org/10.1016/j.biopsych.2008.10.015 (PubMed PMID: 19027102; PubMed Central PMCID: PMC2677389).

Konrad, K., Eickhoff, S.B., 2010. Is the ADHD brain wired differently? A review on structural and functional connectivity in attention deficit hyperactivity disorder. Hum. Brain Mapp. 31 (6), 904–916. http://dx.doi.org/10.1002/hbm.21058 (Epub 2010/05/25. PubMed PMID: 20496381).

Barkley, R.A., 1997. Behavioral inhibition, sustained attention, and executive functions: constructing a unifying theory of ADHD. Psychol. Bull. 121 (1), 65–94 (PubMed PMID: 9000892).

Willcutt, E.G., Doyle, A.E., Nigg, J.T., Faraone, S.V., Pennington, B.F., 2005. Validity of the executive function theory of attention-deficit/hyperactivity disorder: a meta-analytic review. Biol. Psychiatry 57 (11), 1336–1346. http://dx.doi.org/10.1016/j.biopsych.2005.02.006 (PubMed PMID: 15950006).

Lawrence, K.E., Levitt, J.G., Loo, S.K., Ly, R., Yee, V., O'Neill, J., et al., 2013. White matter microstructure in subjects with attention-deficit/hyperactivity disorder and their

siblings. J. Am. Acad. Child Adolesc. Psychiatry 52 (4), 431–440. http://dx.doi.org/10.1016/j.jaac.2013.01.010 (e4; PubMed PMID: 23582873; PubMed Central PMCID: PMC3633105).

Alexander, G.E., DeLong, M.R., Strick, P.L., 1986. Parallel organization of functionally segregated circuits linking basal ganglia and cortex. Annu. Rev. Neurosci. 9, 357–381. http://dx.doi.org/10.1146/annurev.ne.09.030186.002041 (Epub 1986/01/01. PubMed PMID: 3085570).

Menon, V., 2011. Large-scale brain networks and psychopathology: a unifying triple network model. Trends Cogn. Sci. 15 (10), 483–506. http://dx.doi.org/10.1016/j.tics.2011.08.003 (PubMed PMID: 21908230).

Amico, F., Stauber, J., Koutsouleris, N., Frodl, T., 2011. Anterior cingulate cortex gray matter abnormalities in adults with attention deficit hyperactivity disorder: a voxel-based morphometry study. Psychiatry Res. 191 (1), 31–35. http://dx.doi.org/10.1016/j.pscychresns.2010.08.011 (PubMed PMID: 21129938).

Hesslinger B, Tebartz van Elst L, Thiel T, Haegele K, Hennig J, Ebert D. Frontoorbital volume reductions in adult patients with attention deficit hyperactivity disorder. Neurosci. Lett. 2002;328(3):319–21. (PubMed PMID: 12147334).

Proal, E., Reiss, P.T., Klein, R.G., Mannuzza, S., Gotimer, K., Ramos-Olazagasti, M.A., et al., 2011. Brain gray matter deficits at 33-year follow-up in adults with attention-deficit/hyperactivity disorder established in childhood. Arch. Gen. Psychiatry 68 (11), 1122–1134. http://dx.doi.org/10.1001/archgenpsychiatry.2011.117 (PubMed PMID: 22065528; PubMed Central PMCID: PMC3554238).

Hoekzema, E., Carmona, S., Ramos-Quiroga, J.A., Richarte Fernandez, V., Picado, M., Bosch, R., et al., 2012. Laminar thickness alterations in the fronto-parietal cortical mantle of patients with attention-deficit/hyperactivity disorder. PLoS ONE 7 (12), e48286. http://dx.doi.org/10.1371/journal.pone.0048286 (PubMed PMID: 23239964; PubMed Central PMCID: PMC3519773).

van Wingen, G.A., van den Brink, W., Veltman, D.J., Schmaal, L., Dom, G., Booij, J., et al., 2013. Reduced striatal brain volumes in non-medicated adult ADHD patients with comorbid cocaine dependence. Drug Alcohol Depend. 131 (3), 198–203. http://dx.doi.org/10.1016/j.drugalcdep.2013.05.007 (PubMed PMID: 23726981).

Wang, J., Jiang, T., Cao, Q., Wang, Y., 2007. Characterizing anatomic differences in boys with attention-deficit/hyperactivity disorder with the use of deformation-based morphometry. AJNR Am J Neuroradiol. 28 (3), 543–547 (PubMed PMID: 17353333).

Sidman, R.L., Rakic, P., 1973. Neuronal migration, with special reference to developing human brain: a review. Brain Res. 62 (1), 1–35 (PubMed PMID: 4203033).

Poelmans, G., Pauls, D.L., Buitelaar, J.K., Franke, B., 2011. Integrated genome-wide association study findings: identification of a neurodevelopmental network for attention deficit hyperactivity disorder. Am. J. Psychiatry 168 (4), 365–377. http://dx.doi.org/10.1176/appi.ajp.2010.10070948 (PubMed PMID: 21324949).

Yang, L., Neale, B.M., Liu, L., Lee, S.H., Wray, N.R., Ji, N., et al., 2013. Polygenic transmission and complex neuro developmental network for attention deficit hyperactivity disorder: genome-wide association study of both common and rare variants. Am J Med Genet B Neuropsychiatr Genet. 162B (5), 419–430. http://dx.doi.org/10.1002/ajmg.b.32169 (PubMed PMID: 23728934; PubMed Central PMCID: PMC4321789).

Roza, S.J., Verburg, B.O., Jaddoe, V.W., Hofman, A., Mackenbach, J.P., Steegers, E.A., et al., 2007. Effects of maternal smoking in pregnancy on prenatal brain development. the generation R study. Eur. J. Neurol. 25 (3), 611–617. http://dx.doi.org/10.1111/j.1460-9568.2007.05393.x PubMed PMID: 17298594.

Villain, N., Fouquet, M., Baron, J.C., Mezenge, F., Landeau, B., de La Sayette, V., et al., 2010. Sequential relationships between grey matter and white matter atrophy and brain metabolic abnormalities in early Alzheimer's disease. Brain 133 (11), 3301–3314. http://dx.doi.org/10.1093/brain/awq203 (PubMed PMID: 20688814; PubMed Central PMCID: PMC3291528).

Gogtay, N., Giedd, J.N., Lusk, L., Hayashi, K.M., Greenstein, D., Vaituzis, A.C., et al., 2004. Dynamic mapping of human cortical development during childhood through early adulthood. Proc. Natl. Acad. Sci. U. S. A. 101 (21), 8174–8179. http://dx.doi.org/10.1073/pnas.0402680101 (PubMed PMID: 15148381; PubMed Central PMCID: PMC419576).

Paus, T., Zijdenbos, A., Worsley, K., Collins, D.L., Blumenthal, J., Giedd, J.N., et al., 1999. Structural maturation of neural pathways in children and adolescents: in vivo study. Science 283 (5409), 1908–1911 (PubMed PMID: 10082463).

Paus, T., 2005. Mapping brain maturation and cognitive development during adolescence. Trends Cogn. Sci. 9 (2), 60–68. http://dx.doi.org/10.1016/j.tics.2004.12.008 (PubMed PMID: 15668098).